Predicting potential of controlled blasting-induced liquefaction using neural networks and neuro -fuzzy system

Fariba Asvar[1] Arash Shirmohammadi Faradonbeh[2], Kazem Barkhordari Bafghi[3*]

[1]Department of civil engineering, Yazd University, Iran

f.asvar@stu.yazd.ac.ir

[2] Department of civil engineering, Yazd University, Iran

a.shirmohamadi@stu.yazd.ac.ir

[3] Department of Civil Engineering, Yazd University, Iran

kbarkhordari@yazd.ac.ir

Abstract

In recent years, controlled blasting has turned into an efficient method for evaluation of soil liquefaction in real scale and evaluation of ground improvement techniques. Predicting blast-induced soil liquefaction by using collected information can be an effective step in the study of blast-induced liquefaction. In this study, to estimate residual pore pressure ratio, first, multi- layer perceptron neural network is used in which error (RMS) for the network was calculated as 0.105. Next, neuro-fuzzy network, ANFIS was used for modeling. Different ANFIS models are created using Grid partitioning (GP), Subtractive Clustering (SCM), and Fuzzy C-means Clustering (FCM). Minimum error is obtained using by FCM at about 0.081. Finally, radial basis function (RBF) network is used. Error of this method was about 0.06. Accordingly, RBF network has better performance. Variables including fine-content, relative density, effective overburden pressure and SPT value are considered as input components and the R_u, residual pore pressure ratio was used as the only output component for designing prediction models. In the next stage the network output is compared with the results of a regression analysis. Finally, sensitivity analysis for RBF network is tested, its results reveal that σ'_{v_0} and SPT are the most effective factors in determining R_u.

Comment [a1]: In response to comment 1 reviewer 2

Comment [a2]: In response to comment 1 reviewer 1

Keywords: Soil liquefaction, Controlled blasting, Pore water pressure, Artificial neural network (ANN), Neuro-fuzzy, Sensitivity analysis.

1. Introduction

Severe incitement such as earthquakes, impacts, vibrations and explosives can cause liquefaction. In this paper, liquefaction is defined as a geotechnical phenomenon that most often occurs in loose saturated sandy soil, due to decreasing shear resistance following increasing pore pressure [1]. Blast, especially subsurface blasts can lead to huge ruptures due to liquefaction. . In 1935, the rupture of the SWIR III dam in Russia occurred by involuntary liquefaction caused by blast operations in its vicinity,

Comment [a3]: In response to comment 3 reviewer 2

* Corresponding Author. Tel: +983531232476, ~~09133595363~~. Fax: +983538200135

therefore, liquefaction reduced soil dam slope from 2:1 to 10:1. Liquefaction due to nuclear tests in the coral reefs of Eniwetok and Bikini in the Pacific Ocean in 1950 was observed with witnesses such as broad and shallow pits, considerable subsidence and sand boils [2]. Another example of liquefaction related incidents can be found in documentation of Charlie et al. [3].

In geotechnical engineering, controlled blasting is used to model soil liquefaction in real scale, in order to improve the ground by densifying sandy soils, to increase bearing capacity and decreasing permeability coefficient, subsidence and even liquefaction potential in liquefiable soil.

Many studies are conducted in this context such as densifying sub-foundation soil of the Franklin Falls dam in New Hampshire [4], densifying loose soils in 40m depth under Jebba dam in Nigeria [5], improving effectiveness of soil reinforcement methods in order to decrease liquefaction in New Zealand [6], evaluating liquefaction potential in relatively dense clay-rich sand deposits [7], considering critical lines in liquefied soil such as pipelines and airport infrastructure [8], in addition, many experimental studies have been conducted regarding blast-induced liquefaction of soil. More information in this regard, are reported in literature e. g. [1, 9-13]. Unlike experimental studies, limited numerical research has been conducted in this regard. Recently, several techniques have been developed for liquefaction modeling. Byrne et al [14,15], used UBC soil liquefaction model in FLAC-2D software to predict soil liquefaction in sand under dynamic centrifuge test. Gohl, [16] used PGI's single-charge 2D blast-induced liquefaction model in the LS-DYNA finite-element software for 2D symmetrical simulation of soil liquefaction caused by single blasts. Taylor and Bell et al [17, 18] , presented Taylor's effective stress material model for saturated soils in the CTH code. Taylor model was specifically suggested for impact loadings with high magnitude similar to short-term blasts to predict soil liquefaction. Unfortunately, Taylor model and CTH code are not commercially available. Lewis [19] developed FHWA's LS-DYNA soil material model 147. This is a scientific accessible model for predicting blast-induced liquefaction of soil. Also, several case studies have been conducted in this context. Wang et al [20] developed three-phase soil model for simulating stress wave propagation due to blast loading. This model has unique ability to simulate blast-inducted liquefaction of soil, but unfortunately is not available commercially. Wang et al [21] conducted numerical simulation of quasi-static test and shock test to investigate liquefaction. Simulation was conducted using three-phase soil model and hydrocode AUTODYN. Wang et al sought to prove ability of three-phase soil model and hydrocode AUTODYN in simulating impact and shock-induced liquefaction of soil. Wang et al [2] performed another numerical study to consider the effect of blast-induced soil liquefaction on surface structure. In this study, three-phase soil model and hydrocode AUTODYN were used. Lee [16] conducted field tests of blast-induced liquefaction in Vancouver to determine soil characteristics under severe and subsequent blasts to simulate big earthquakes. He simulated the relevant tests using LS-DYNA finite element software.

Amount of pore water pressure is a key factor in liquefaction. Based on review of technical literature and available sources, several experimental models have been presented to predict pore pressure response due to blasting.

Comment [a4]: In response to comment 2 reviewer 1

Comment [a5]: In response to comment 3 reviewer 1

Comment [a6]: In response to comment 5 reviewer 2

Comment [a7]: In response to comment 4 reviewer 1 and comment 7 reviewer 2

Comment [a8]: In response to comment 11 reviewer 2

Experimental models of Charlie et al, Kummeneje et al and Studer et al [22-24] for single blast and Rollins model [25] as cited by [26] were introduced for multiple blasts. The experimental models suggested by researchers except that of Kummeneje et al [23] do not consider soil characteristics in prediction R_u.

Performance field blast tests in real scale have high costs and many limitations. Moreover, results of experimental models show great dependency to site conditions and experiment method. Under these conditions, statistical methods and AI-based methods (artificial neural networks and fuzzy systems) with available data have opened up a new world for researchers. Artificial neural network and neuro-fuzzy system despite its low cost (relative to experimental methods used to predict blast-induced liquefaction), is an efficient and reliable method in data processing even despite various effective parameters and their complex relations.

Eller [26], by multiple regression analysis considered predicting pore pressure response in liquefaction studies by using controlled blasting.

The artificial neural networks and neuro-fuzzy system has not bring substantial development for prediction of blast-induced liquefaction potential. The Neural network is a powerful prediction tool and is more accuracy than other conventional methods for complex problems such as liquefaction, where the relationship between variables is not clear [27]. Artificial neural networks are used in various geotechnical fields such as liquefaction [28-30], soil behavior modeling, earth retaining structures, predicting bearing capacity of piles, settlement of structures, slope stability, designing tunnels, and hydraulic conductivity of soil [31]. Another appropriate method in prediction of liquefaction potential is neuro-fuzzy systems. It is a combination of neural networks and fuzzy logic determines parameters of fuzzy systems using neural network training algorithm [32]. Fuzzy systems has successful application in geotechnical problems such as prediction of unconfined compressive strength of compacted granular soils [33], prediction of foundation response [34], swelling potential of compacted soil [35], estimation of sand permeability [36], and evaluation of liquefaction potential [37]. Other neuro-fuzzy applications were reported by Cabalar at el[37].

The present study aims to predict blast-induced liquefaction potential using multi layer perceptron neural networks (MLP), radial basis functions (RBF), and the neuro-fuzzy (NF) model and comparing efficiency of these methods. Furthermore, sensitivity analyses on input network variables have been carried out to identify effective parameters in liquefaction

2. Materials and Methodology

2.1. Datasets collected

In this study, data required for designing neural networks and neuro-fuzzy system are obtained from results of multiple blasts in real scale performed in seven different parts of the world (1997-2007) as cited by Eller[26].

Following is a brief description of the experiments:

1. Controlled blast for inducing liquefaction with the purpose of evaluating seismic performance of Japanese airport infrastructures in 2007 [38,39].

Comment [a9]: In response to comment 8 reviewer 1

Comment [a10]: In response to comment 12 reviewer 2\

Comment [a11]: In response to comment 9 reviewer 1

Comment [a12]: In response to comment 10 reviewer 1

Comment [a13]: In response to comment 11 reviewer 1

Comment [a14]: In response to comment 13 reviewer 2

Comment [a15]: In response to comment 13 reviewer 2

Comment [a16]: In response to comment 14 reviewer 2

Comment [a17]: In response to comment 15 reviewer 2

2. Controlled blasting for evaluating performance of vertical composite earthquake drains for reducing potential of liquefaction caused by earthquake in 2004 in the vicinity of Massy Tunnel in Vancouver [40, 41].

3. Experiment for evaluating liquefaction potential of Coralline sands in 2004 in Mawi, Hawaii [25].

4. Blast experiment for evaluating performance of piles, pipelines and quay walls against lateral spreading of static and seismic load in Japan (2002) [42].

5. Testing blast-induced liquefaction with the purpose of investigating liquefaction potential of problematic soils such as low-plasticity silts in Canada (2000) [11].

6. Blast testing to improve deep foundations design under lateral loadings caused by earthquake in San Francisco, California (1998) [9, 43, 44].

7. Controlled blasting for simulating earthquake-induced ground movements in Canada (1997) [45].

2.2. Neural network models

2.2.1. Multi layer perceptron networks

Perceptron network or MLP is one of the mostly used neural networks. This network consists of three layers i.e. input, hidden and output. The MLP network is a feed forward network with back propagation training procedure. Back propagation means that after determining the network output, if there is a difference between obtained output and desired output, first weights of the last layer are corrected and then weight correction procedure goes toward input layers [46]. To determine network coefficients, Levenberg -Marquardt (LM) algorithm [47] was used. This algorithm is considered a classic method for optimization. Data are entered to the network in normalized form in three parts of training (70%), validation (15%), and testing (15%). Number of hidden layers and neurons of every layer is obtained via trial and error to minimize network error. MLP optimal network is shown in figure 1. In hidden and output layers the tansig transfer function is used due to continuity and differentiability. A summary of MLP parameters and specifications is shown in table 1.

Insert Figure1

Insert Table1

2.2.2. Fuzzy system

The Fuzzy system was first proposed by Zadeh [48]. In classic logic, truth value of a proposition is either 0 or 1, while in fuzzy logic truth value of a proposition can be a value between zero and one. In fact, propositions can be relatively true [37]. Neural networks function based on data whose pattern is not known. Fuzzy rules are expressed in IF-THEN form [37].

Two types of Fuzzy inference systems have been used in various applications such as: Mamdani and Takagi-Sugeno-Kang (TSK). In the Mamdani system both the antecedent and consequent of rules are expressed as fuzzy sets, while in the Sugeno system antecedent part of rules is fuzzy,

Comment [a18]: In respose to comment 16 reviewer 2

Comment [a19]: In response to comment 15 reviewer 1

Comment [a20]: In response to comment 16 reviewer 1

Comment [a21]: In response to comment 17 reviewer 1

the consequent part is non-fuzzy and in form of accurate mathematical relationship of linear combination of input variables. For fuzzy system with two inputs x and y and output z, used the eqns (1) are used as per [37]in Eq. (1) [37]:

Comment [a22]: In response to comment 17 reviewer 2

Rule 1: If x is A_1 and y is B_1, then $f_1 = p_1x + q_1y + r_1$ (1.a)

Rule 2: If x is A_2 and y is B_2, then $f_2 = p_2x + q_2y + r_2$ (1.b)

where p_i, q_i and r_i are consequent parameters of i_{th} rule. A_i, B_i and C_i are linguistic labels representing fuzzy sets shown in figure 2.

Insert figure 2

In this study, Sugeno fuzzy inference system (FIS) has been used. The inference process in Sugeno fuzzy system is performed in three main steps [37]:

A. Determining membership degree of input data: In other words, fuzzification of input signals using membership functions

B. Determining weight of every rule: In this stage, the relationship between input and output is expressed with rules such as IF-THEN.

C. Determining system output: Output is determined in non-fuzzy form using OR and AND operators.

2.2.3. Neuro-fuzzy system

Neuro-fuzzy system was first introduced by Jang [32]. This method is a combination of fuzzy logic and neural network training methods. The neuro-fuzzy system used in this study, ANFIS (adaptive neuro-fuzzy inference system) is a Sugeno-type neuro-fuzzy inference system.

In this study, the ANFIS model was created in three methods of grid partitionig (GP), subtractive clustering (SCM) and fuzzy c-means clustering (FCM). In GP, every part of premise variables is suggested independently. To develop this expert model, membership functions of all premise variables are defined based on former knowledge and experience. Membership functions are designed to create concept for linguistic expressions in certain content. In most systems no special knowledge is available for this classification. In such cases, the domain of antecedent variables can simply be classified into equal spaces and membership functions with equal forms. Using available input-output data, membership function parameters can be adjusted and optimized. The SCM method was first introduced by Chiu [49]. When number of clusters that should be chosen for data sets is not clear, SCM is a quick method for determining number of clusters and their centers.

The FCM method was first introduced by Bezdek (1981) [50] and is the most popular fuzzy clustering technique. FCM has improved SCM performance. In this method, data are grouped based on their degree of membership. FCM has improved SCM performance [51].

Comment [a23]: In response to comment 18 reviewer 1

Collected information is classified into two sets of training and testing. 335 data items (80% of data) were considered in train stage and 81 data items (20% of data) were considered for test.

2.2.4. Radial basic function networks

A radial basis function network (RBF) is a function in which every output is produced corresponding to desired input and with a certain radial distance [52]. Figure 3 schematically shows RBF network. It is a type of mono-layer neural networks. Inputs enter the hidden layer space with a non-linear mapping. Output of cells in hidden layer after being multiplied by related weights enter an adder which is output for the neural network. The RBF function can be defined in the form of following mathematical Eq. (2):

Insert Figure 3

$$y = w.\phi(\mathrm{x}) = w^T \phi(\mathrm{x}) \qquad (2)$$

where y is network output and φ is activation function. These functions strongly influence network performance, taking input to the hidden space. The activation function used in design of RBF network is Gaussian function which is shown in Eq. (3) and Eq. (4) [53]:

$$\phi(\mathrm{x}) = (\phi_1(\mathrm{x}), \phi_2(\mathrm{x}), \dots, \phi_M(\mathrm{x}))^T \qquad (3)$$

$$\phi_i(\mathrm{x}) = \exp\left(\left\| x - c_i \right\|^2\right) \qquad (4)$$

Where c_i denotes center of Gaussian function which is better to be chosen from data. x is input variable. 80% of available data (333 data items) are considered for network training and 20% (83 data items) are considered for experiment. The root mean square error algorithm (RMSE) is used for training. Network training continues until error of total squares is less than the specified target error or until maximum specified neuron count is reached. The error that we expect the network to reach is 0.007. Assumed neuron count is equal to the default value.

3. Input and output parameters

3.1. Input parameters

Input parameters to neural network are chosen in such a way to have appropriate overlapping in evaluating blast-induced liquefaction potential. Four factors influence residual pore pressure ratio (evaluation criterion of soil liquefaction). These factors include: soil type, soil density, soil saturation degree and vibration magnitude [26]. Table 2 shows range of changes for input and output variables.

Insert Table 2

On this basis, parameters affecting liquefaction potential (parameters input to the neural network) are used as follows:

1. Scaled distance ($R/W^{0.33}$): In this study, Hopkinson of scaled distance, Eq. (4) and Eq. (5) [16] has been used to express specification of blast load (amount of energy needed for liquefaction):

$$SD = R/W^{0.33} \qquad (5)$$ For Single explosions

Comment [a24]: In response to comment 18 reviewer 1

$$R/W^{0.33} = \frac{\bar{R}}{\sum W^{0.33}} = \frac{\left(\frac{R_1 + R_2 + ... + R_i}{N_I}\right)}{\sum\left(W_1 + W_2 + ... + W_i\right)^{0.33}} \quad (6)$$

For Subsequent explosions

Comment [a25]: In response to comment 19 reviewer 1

where W and W_i are weight of TNT explosive and R is the distance between explosive and point of observation.

2. SPT $(N_1)_{60}$ value,
3. Effective overburden pressure: $\sigma'_{v_0}\,(Kpa)$
4. Initial relative density: D_R (%)
5. Fine content: FC (%)

3.2. Output parameter

To evaluate potential of liquefaction due to earthquake various criteria is provided. Some of these criteria are cyclic shear stress [54], cyclic shear strain [55] and energy required for soil liquefaction [37], which was used as evaluation criteria predicting liquefaction. Typical criterion used to investigate blast-induced soil liquefaction is to use the residual pore pressure ratio, R_u [26, 21, 16, 2]. In this study R_u has been used as the only output parameter according to Eq. (7):

$$R_u = \frac{\Delta u}{\sigma'_{v_0}} \quad (7)$$

Δu is residual pore pressure. In non-drained conditions, increased R_u leads to decreased σ'_{v0}, when $R_u = \sigma'_{v0}$, the soil loses its shear resistance and liquefaction occurs. R_u greater than zero means excess pore pressure in soil and $R_u = 1$ means occurrence of complete soil liquefaction [28]. Given the above criterion, the following conditions are considered when evaluating soil liquefaction [2]:

1. $\frac{\Delta u}{\sigma'_{v_0}} = 0.1$ is considered as secure range (based on conducted experiments, in some cases up to $\frac{\Delta u}{\sigma'_{v_0}} = 0.6$ be allowed).
2. $\frac{\Delta u}{\sigma'_{v_0}} = 0.8$ has been assumed as dangerous range.
3. $\frac{\Delta u}{\sigma'_{v_0}} \geq 1$ shows the range where contact between soil granules disappears; soil loses its shear resistance and liquefaction occurs.

Neural network training using raw data results in reduced network speed and accuracy. Thus, to achieve desired error level, data were standardized before entering the network using Eq. (8) [56]:

$$x_N = \frac{\left(x - x_{\min}\right)}{\left(x_{Max} - x_{\min}\right)} \quad (8)$$

where x_N is normalized value of x, x_{Max} maximum and x_{min} minimum value for every variable.

4. Evaluation criteria

To evaluate efficiency of neural network models and compare their effectiveness the following statistical indicators have been used:

1. Correlation coefficient (R^2): represents degree of relationship between predicted values of neural network and observed values:

$$R^2 = \frac{\sum_{i=1}^{n}\left(\tilde{y}_i - \bar{y}\right)^2}{\sum_{i=1}^{n}\left(y_i - \bar{y}\right)^2} \quad (9)$$

Where y_i is observed values, $\tilde{y}_i$ is computed values and $\bar{y}$ is mean of observed values.

2. Root mean square error (RMSE): shows difference between value predicted by network and actual value:

$$RMSE = \sqrt{\frac{1}{n}\sum_{i=1}^{n} e_i^2} \quad (10.1)$$

$$e_i = y_i - \tilde{y}_i \quad (10.2)$$

where e_i is the error between actual value and predicted value.

3. Mean absolute error (MAE):

$$MAE = \frac{1}{n}\sum_{i=1}^{n} e_i \quad (11)$$

4. Maximum absolute error (MAX):

$$MAXAE = Max(|e_i|) \quad (12)$$

Using the following indicators, the ability of network in identifying liquefaction incident can be investigated.

The parameters given in equations 9 to 12 for this study are given as follows:

Positive (1): conditions when soil is liquefied and negative (0): condition when soil is secure (non-liquefied). TP=true positive: number of liquefaction samples which were correctly reported as liquefied soil. TN=true negative: number of non-liquefied samples which were reported as soil without liquefaction conditions. FP=false positive: number of non-liquefied samples which were falsely reported as liquefied soil. FN=false negative: number of liquefied samples falsely reported as non-liquefied soil. Meaning of these parameters can be expressed in the following table 3:

Insert Table 3

5. TPR: (sensitivity), percentage of liquefied samples which were truly reported as soils having liquefaction conditions.

True positive ratio (TPR) =Sensitivity=Recall= TP/ (TP+FN) (13)

6. PPV: (accuracy): percentage of samples for which the predicted liquefaction conditions are true.

Positive predictive value (PPV) =Precision=TP (TP+FP) (14)

7. TNR: (characteristic): percentage of non-liquefied samples truly reported as safe soil (non-liquefied).

True negative rate (TNR) =Specificity= $\frac{TN}{TN+FP}$ (15)

8. Accuracy: percentage of samples for which liquefaction and non-liquefaction conditions were properly predicted.

ccuracy = (16)

$$\frac{TN+TP}{TN+FP+TP+FN}$$

5. Results and Discussion

5.1. MLP

In this study, to calculate R_u, different models of MLP were created to determine optimal number of neurons in hidden layers and transfer functions. In figure 4 training curve for selective MLP network with two hidden layers is given. By investigating the above figure, the following results follow:

1.Mean square error is small 2. Error of experiment set shows a behavior similar to that of evaluation set. 3. No fitting has occurred until iteration 21.

Insert Figure 4

To evaluate MLP network performance regression coefficient figure for training and testing data is drawn in figure 5 and evaluation criterion for MLP model is shown in table 4. For test data, the network has produced three incorrect predictions (accuracy=0.952). In two cases where soil was liquefied, the network had predicted non-liquefaction and in one case the prediction was opposite to this.

Comment [a26]: In response to comment 23 reviewer 1

Comment [a27]: In response to comment 19 reviewer 1

Insert Figure 5

Insert Table 4

5.2 ANFIS

ANFIS is the second prediction model which is used in this study and results are reported. figure of correlation coefficient for three different algorithms of ANFIS is shown in figures 6 to 8. The most coefficient for training datasets were obtained via GP ($R^2 = 0.935$) and for testing datasets via FCM ($R^2 = 0.931$). Index values of evaluation for three methods are provided in table 5. Given the results shown in the table, the first point to consider is that GP method performed better compared with the two other methods for training dataset, while FCM shows better performance for test

Comment [a28]: In response to comment 24 reviewer 1 and comment 20 reviewer 2 data. Predictions made by GP, SCM and FCM were incorrect in 9, 3, and 1 cases respectively. Therefore, the best performance in detecting incidence or non-incidence of liquefaction pertained to FCM and then to SCM. GP performed more poorly than the two other methods.

Insert Figure 6

Insert Figure 7

Insert Figure 8

Insert Table 5

5.3. RBF

Besides MLP and ANFIS another type of neural network called RBF was used. To bring balance between accuracy and training time the target error (goal) was considered to be 0.007. The consider prediction quality of RBF model for training and testing data sets, actual values of R_u is drawn versus network prediction values in figure 9. Also, in table 6 evaluation criterion for RBF model is shown. From the table results it could be inferred that network error for both datasets is little (RMS (train) =0.088, RMS (test) =0.060). Also, all error criteria for testing have been obtained less than training. Using the criterion given in table 6 RBF performance in detecting incidence or non-incidence of liquefaction can be evaluated. Network accuracy for test data was 0.98 which shows its good performance. In fact, for 98% of test data correct prediction has been performed. Only in one case where soil was liquefied (R_u=0.94) the network prediction was non-incidence of liquefaction (R_u=0.68). High values of correlation coefficient ($R^2(test) = 0.942, R^2(train) = 0.915$) show good relationship between predicted values of R_u and observed values.

Insert Figure 9

Insert Table 6

6. Comparison of Neural Network Results with Field Results and Eller Regression Analysis

Based on regression analysis using datasets used for designing neural networks, an equation has been obtained by Eller [26] for calculating residual pore pressure ratio caused by blast-load. To evaluate performance for a given network, its output along with observed data and results of regression analysis are provided in table 7. In columns 2,4, and 6 liquefaction potential of soil in all three mentioned cases is given. As seen from the results of table 7, the network has more accuracy than regression analysis. As it is observed, in detecting soil liquefaction potential for 83 test data item (table 7 data), the network is incorrect in one item and regression is incorrect in 10 items.

Insert Table 7

7. T-Test

To compare mean of a quantitative variable in two groups, t-test is used. In this study, for two datasets, the R_u observed from experiments and R_u from network prediction, t-test was performed with the results displayed in table 8. Given the values of table, critical t-value for 95% probability is 1.97. As observed, the calculated value is less than the critical value. Therefore, results of t-test show that with 95% confidence interval, no considerable difference exists between these two groups.

Insert Table 8

8. Sensitivity Analysis

Parameters mentioned regarding soil specification (network input parameters) include: SPT value, effective overburden pressure, relative density and fine content. To consider the effect of these parameters on residual pore pressure ratio, sensitivity analysis using RBF network was done. The reason for using RBF network is that the analysis results of this model are better than two networks of ANFIS and MLP. Analysis results are given in table 9. As it is observed, maximum error is for the case where SPT parameter is removed. This means SPT is the most effective parameter in determining R_u. The second effective factor is σ'_{v0}. D_R and FC parameters compared with two other parameters have smaller effect on network output.

Comment [a29]: In response to comment 22 reviewer 2

Insert Table 9

. Conclusion

In this paper, using MLP and RBF neural networks and ANFIS model, values of pore water pressure response due to blasting were estimated. Five input variables and one output variable were used for designing prediction models. Best structure for all three networks was selected based on trial and error. For MLP network best model was obtained with two hidden layers, 15 neurons in first hidden layer and 5 neurons in the second hidden layer (5-15-5-1). The ANFIS neuro-fuzzy model was tested with three algorithms of FCM, SCM and GP. Among neuro-fuzzy models constructed, FCM, SCM, and GP had a better performance in terms of prediction quality and the time required for solving. GP model was very slow. It is recommended that for problems with 5 and more input components (as in the present study) FCM and SCM methods should be used. That is because as input variables increase, number of fuzzy rules created in the GP model increase exponentially.

Comment [a30]: In response to comment 23 reviewer 2\

Comment [a31]: In response to comment 23 reviewer 2\

Results of this study show that for all evaluation criteria, RBF has the highest accuracy and ANFIS (GP) has the lowest accuracy in predicting the results. Networks designed in this paper are in following order based on above mentioned evaluation criteria based on their performance: RBF, ANFIS (FCM), ANFIS (SCM), MLP, ANFIS (GP) respectively.

Networks ability to predict incidence or non-incidence of liquefaction was investigated using accuracy, TPR, PPV and TNR criteria. For RBF and ANFIS (FCM), identical results were obtained.

In the next stage of the study, network output was compared with actual values and formula obtained from statistical analysis. Neural networks can provide predictions with smaller errors than conventional regression methods. In fact, it could be suggested that the network has shown an acceptable performance in data simulation.

Also t-test was done between observed and predicted data. Results showed that assumption on equality of means with 95% probability is confirmed. Finally, sensitivity analysis was carried out for RBF (most suitable model) in order to identify the most effective parameters in production of pore water pressure. Results of sensitivity analysis showed that SPT number is the most effective parameter.

While the designed models have appropriate performance, the results could be improved by increasing the number of data. Neural network model can be a suitable tool for evaluating potential of soil liquefaction caused by blast loads.

Comment [a32]: In response to comment 25reviewer 1

Comment [a33]: In response to comment 24 reviewer 2\

References

1. Charlie, W.A., Bretz, T.E., Schure (White), L.A. and Doehring, D.O. “Blast-induced pore pressure and liquefaction of saturated sand”, J. Geotech. Geoenviron. Eng., 139, pp. 1308-1319, DOI: 10.1061/ (ASCE)GT.1943-5606.0000846 (2013).

2. Wang, Z., Lu, Y. and Bai, C. “Numerical simulation of explosion-induced soil liquefaction and its effect on surface structures”, Journal of the Finite Elements in Analysis and Design., 47, pp. 1079–1090, DOI:10.1016/j.finel.2011.04.001 (2011).

3. Charlie, W.A., Hubert, M.E., Schure, L.A.,Veyera, G.E. and et al. “Blast-induced soil liquefaction: summary of literature”, Final Report to AFOSR, AD-A19995, Department of Civil Engineering, Colorado State University (1988).

4. Lyman, A.K.B. “Compaction of cohesionless foundation soils by explosives”, Transactions ASCE (107) pp. 1330 – 1348. (1942).

5. Solymar, S.V. “Compaction of alluvial sands by deep blasting”, Can. Geotech. J., 21(2), pp. 305 – 321 (1984).

6. Kato, K., Mason, H.B. and Ashford, S.A. “Ground vibration from blast-induced liquefaction testing in Christchurch, New Zealand”, 6th International Conference on Earthquake Geotechnical Engineering., Christchurch, New Zealand (2015).

7. Hatzor, Y.H., Gvirtzman, H., Wainshtein, I, and Orian, I. “Induced liquefaction experiment in relatively dense, clay-rich sand deposits”, J. Geophys. Res, B02311., 114, pp. 1–22 (2009). DOI:10.1029/2008JB005943.

8. Sugano, T., Kohama, E., Mitoh, M. and Shiozaki, Y. “Seismic performance of urban, reclaimed and port areas – full scale experiment at

Tokachi port by controlled blasting technique”, The Earthquake Engineering Symposium, 11, pp. 901 – 906. (2002).

9. Ashford, S.A., Rollins, K.M. and Lane, J.D. “Blast-induced liquefaction for full-scale foundation testing”, J. Geotech. Geoenviron. Eng., 130(8), pp. 798 – 806 (2004).

10. Bolton, J.M., Durnfold, D.S. and Charlie, W.A. “ One-dimensional shock and quasi-static liquefaction of silt and sand”, J. Geotech. Engrg., 120(10), pp. 1889 – 1974 (1994).

11. Gohl, W.B., Howie, J.A. and Rea, C.E. “Use of controlled detonation of explosives for liquefaction testing”, Fourth Int. Conf. On Recent Advances in Geotechnical Earthquake Engineering and Soil Dynamics, San Diego, Calif., paper no. 913. USA (2001).

12. Rollins, K.M., Gerber, T.M., Lane, J.D. and Ashford, S.A. “Lateral resistance of a full-scale pile group in liquefied sand” J. Geotech. Geoenviron. Eng,. 131(1), pp. 115–125(2005).

13. Hijikata, K., Ishida, T., Tanaka, H., Koyamada, K., Miyamoto, Y., Kontani, O. and Nigbor, R. “Experimental study on soil-pile-structure interaction in liquefiable sand subjected to blast-induced ground motion”, 13th World Conference on Earthquake Engineering., Vancouver, B.C., Canada, Paper No. 190 (2004).

14. Byrne, P.M., Park, S.S., Beaty, M., Sharp, M., Gonzalez, L. and Abdoun T. “Numerical modeling of liquefaction and comparison with centrifuge tests”, Can. Geotech. J., 41, pp. 193-211 (2004).

15. Byrne, P.M., Park, S.S., Beaty, M., Sharp, M., Gonzalez, L., and Abdoun T. “Numerical modeling of dynamic centrifuge tests”, 13th World Conference on Earthquake Engineering. Vancouver, B.C., Canada, Paper No. 3387 (2004).

16. Lee, W.Y. “Numerical modeling of blast-induced liquefaction”, PhD thesis, Department of Civil and Environmental Engineering, Brigham Young University, 67(06B):3305 (2006). 17. Taylor, P.A. “Modeling the response of variably saturated geomaterials to large strain rate loading”, Department of Computational Physics & Simulation Frameworks Presentation. Sandia National Laboratories. Albuquerque, NM, USA (2004).

18. Bell, R.L., Baer M.R., Brannon, R.M., Crawford, D.A., Elrick, M.G., Hertel, E.S.Jr., Schmitt, R.G., Silling, S.A. and Taylor P.A. “CTH user’s manual and input instructions”, Version 7.0. Sandia National Laboratories, Albuquerque, NM, USA (2005).

19. Lewis, B.A. “Manual for LS-DYNA soil material model 147”, Report FHWA-HRT-04-095, McLean, VA, Federal Highway Administration (2004).

20. Wang, Z., Hao, H. and Lu, Y. “A three-phase soil model for simulating stress wave propagation due to blast loading”, Int. J. Numer. Anal. Meth. Geomech., 28, pp. 33–56, DOI: 10.1002/nag.325 (2004).

21. Wang, Z., Lu, Y. and Bai, C. “Numerical analysis of blast-induced liquefaction of soil”, Comput. Geotech., 35 (2), pp. 196 – 209, DOI: 10.1016/j.compgeo.2007.04.006 (2008).

22. Charlie, W.A. and Doehring, D.O. “Groundwater table mounding, pore pressure, and liquefaction induced by explosions: Energy-Distance Relations”,
Rev. Geophys., 45, RG4006. pp. 1– 9 (2007).

23. Kummeneje, O. and Eide, O. “Investigation of loose sand deposits by blasting”, 5th International Conf. Soil Mechanics and Foundation Engineering, 1, pp. 491– 497 (1961).

24. Studer, J. and Kok, L. “Blast-induced excess porewater pressure and liquefaction experience and application”, International Symposium on Soils under Cyclic and Transient Loading, Swansea, UK, pp. 581 – 593 (1980).

25. Rollins, K.M., Lane, J.D., Nicholson, P.G. and Rollins, R.E. “Liquefaction hazard assessment using controlled-blasting techniques”, 11th International Conference on Soil Dynamics & Earthquake Engineering, 2, pp. 630 – 637 (2004).

26. Eller, J.M. “Predicting pore pressure response in in-situ liquefaction studies using controlled blasting”, Master’s thesis, Oregon State University (2011).

27. Baziar, M.H. and Ghorbani, A. “Evaluation of lateral spreading using artificial neural networks”, Soil Dynamics and Earthquake Engineering, 25(1), pp. 1-9, DOI:10.1016/j.soildyn.2004.09.001 (2005).

28. Hanna, A.M., Ural, D. and Saygili, G. “Neural network model for liquefaction potential in soil deposits using Turkey and Taiwan earthquake data”, Soil Dynamics and Earthquake Engineering, 27(6), pp. 521-540, DOI:10.1016/j.soildyn.2006.11.001 (2007).

29. Juang, C.H., Chen, C.J. and Tien, Y-M. “Appraising cone penetration test based liquefaction resistance evaluation methods: artificial neural network approach”, Can. Geotech. J., 36(3), pp.443–454, DOI: 10.1139/t99-011 (1999).

30. Juang, C.H., Chen, C.J., Jiang, T. and Andrus R.D. “Risk-based liquefaction potential evaluation using standard penetration tests”, Can. Geotech. J., 37(6), pp. 1195–208, DOI: 10.1139/t00-064 (2000).

31. Shahin, M.A., Jaksa, M.B. and Maier H.R. “Artificial neural network applications in geotechnical engineering”, Australian Geomechanics, 36(1), pp. 49-62 (2001).

32. Jang, J.S.R., Sun, CT. and Mizutani, E. “Neuro-fuzzy and soft computing: a computational approach to learning and machine intelligence”, Prentice Hall, New Jersey, USA (1997).

33. Kalkan, E., Akbulut, S., Tortum, A. and Celik, S. “Prediction of the unconfined compressive strength of compacted granular soils by using inference systems”, Environ. Geol., 58, pp. 1429–1440, DOI: 10.1007/s00254-008-1645-x (2008).

34. Provenzano, P., Ferlisi, S. and Musso, A. “Interpretation of a model footing response through an adaptive neural fuzzy inference system”, Comput. Geotech., 31, pp. 251–66 (2004).

35. Kayadelen, C., Taskiran, T., Gunaydin, O. and Fener, M. “Adaptive neuro-fuzzy modeling for the swelling potential of compacted soils”, Environ. Earth Sci., 59, pp. 109-115 (2009).

36. Sezer, A., Goktepe, B.A. and Altun, S. “Adaptive neuro-fuzzy approach for sand permeability estimation”, Environ. Eng. Manage. J., 9(2), pp. 231–238 (2010).

37. Cabalar, A.F., Cevik, A. and Gokceoglu, C. “Some applications of Adaptive Neuro-Fuzzy Inference System (ANFIS) in geotechnical

engineering", Comput. Geotech., 40, pp. 14–33, DOI:10.1016/j.compgeo.2011.09.008 (2012).

38. Nakazawa, H., and Sugano, T. "Full-scale field test on liquefaction-induced damage of runway pavement by controlled blast technique", 9th U.S. National Conference on Earthquake Engineering, Toronto, Ontario – Canada, (2010).

39. Port and Airport Research Institute (PARI), Japan. "Full-scale field experiment of airport facilities during liquefaction induced by controlled blasting technique", Technical Note of the Port and Airport Research Institute. Independent Administrative Institution, Japan, 338 pp (2009) (In japanese).

40. Rollins, K.M. "Liquefaction mitigation using vertical composite drains: full scale testing", Final Report for Highway IDEA Project 94. Transportation Research Board, 105 pp (2004).

41. Strand, S.R. "Liquefaction mitigation using vertical composite drains and liquefaction-induced downdrag on piles: implications for deep foundation design", PhD thesis, Department of Civil and Environmental Engineering, Brigham Young University (2008).

42. Ashford, S.A. and Juirnarongrit, T. "Performance of lifelines subjected to lateral spreading", Report SSRP-04/18, Department of Structural Engineering, University of California, San Diego (2004).

43. Ashford, S.A., Juirnarongrit, T., Sugano, T. and Hamada, M. "Soil-pile response to blast-induced lateral spreading.1: field test", J. Geotech. Geoenviron. Eng., 132(2), pp. 152 – 162, DOI: 10.1061/(ASCE)1090-0241(2006)132:2(152), (2006).

44. Ashford, S.A. and Rollins, K.M. "TILT: Treasure island liquefaction test: final report", Report SSRP-2001/17, Department of Structural Engineering, University of California, San Diego (2002).

45. Pathirage, K.S. "Critical assessment of the CANLEX blast experiment to facilitate a development of an in-situ liquefaction methodology using explosives", Master's thesis, Department of Civil Engineering, The University of British Columbia (2000).

46. Emami, M. "Application of artifitial neural networks in pressuremeter test results", Master's thesis, Tarbiat Modares University, Tehran, Iran (2009).

47. Marquardt, D.W. "An algorithm for least squares stimation of nonlinear parameters", Soc. Ind. Appl., 11(2), pp. 431-441, DOI:10.1137/0111030, (2006).

48. Zadeh, L.A. "Fuzzy sets", Inform. Control., 8 pp. 338–53 (1965).

49. Chiu, S.L. "Fuzzy model identification based on cluster estimation", Journal of Intelligent & Fuzzy Systems, 2, pp. 267-278 (1994).

50. Bezdek, J.C. "Pattern Recognition with Fuzzy Objective Function Algorithms", Advanced application in pattern recognition, Plenum Press, New York and London, DOI: 10.1007/978-1-4757-0450-1, (1981).

51. Behnia, D., Ahangari, K., Noorzad, A. and Moeinossadat, S.R. "Predicting crest settlement in concrete face rockfill dams using adaptive neuro-fuzzy inference system and gene expression programming intelligent methods", J. Zhejiang. Univ-Sci. A. (Appl. Phys & Eng)., 14(8), pp. 589-602, DOI:10.1631/jzus.A1200301 (2013).

52. Gupta, M.M., Jin L. and Homma N. “Static and Dynamic Neural Network”, From Fundamentals to Advanced Theory, A John Wiley & Sons, INC., Publication, Hobokon, New Jersey (2003).

53. Fyfe, C. “Artificial neural networks”, Department of Computing and Information Systems, The University of Paisley, Room, 1.1 Edn., (1996).

54. Seed, H.B. and Idriss I.M. “Simplified procedure for evaluating soil liquefaction potential”, J. Soil. Mech. Found. Div., ASCE, 97(SM9), pp. 1249–1273 (1971).

55. Dobry, R., Ladd, R.S., Yokel, F.Y., Chung, R.M. and Powell, D. “Prediction of pore water pressure buildup and liquefaction of sands during earthquakes by the cyclic strain method”, Build. Sci. Series., 138, National Bureau of Standards, US Department of Commerce, US Governmental Printing Office, Washington, DC (1982).

56. Emamgholizadeh, S., Kashi, H., Marofpoor, I. and Zalaghi, E. “Prediction of water quality parameters of Karoon River (Iran) by artificial intelligence-based models”, Int. J. Environ. Sci. Technol., 11, pp. 645-656, DOI: 10.1007/s13762-013-0378-x, (2014).

Legends for the Figures and Tables

Figure 1 Optimal model of MLP perceptron network.

Figure 2 The Sugeno fuzzy model [37].

Figure 3 Structure of RBF network.

Figure 4 MLP network training curve.

Figure 5 Scatter plots of measured and predicted Ru (residual pore pressure ratio values) using MLP. (a) Training set. (b) Testing set.

Figure 6 Scatter plots of measured and predicted Ru (residual pore pressure ratio values) using (ANFIS (GP)). (a) Training set. (b) Testing set.

Figure 7 Scatter plots of measured and predicted Ru (residual pore pressure ratio values) using (ANFIS (SCM)). (a) Training set. (b) Testing set.

Figure 8 Scatter plots of measured and predicted Ru (residual pore pressure ratio values) using (ANFIS (FCM)). (a) Training set. (b) Testing set.

Figure 9 Scatter plots of measured and predicted Ru (residual pore pressure ratio values) using RBF. (a) Training set. (b) Testing set.

Table 1 Features of the proposed MLP model.

Table 2 Ranges of input and output variables with basic statistics.

Table 3 Definition of FN, FP, TN and TP parameters.

Table 4 Evaluation criteria for MLP.

Table 5 Evaluation criteria for ANFIS network.

Table 6 Evaluation criteria for RBF network.

Table 7 Comparison of network simulation with field results and regression analysis.

Table 8 Investigation of neural network model compared to actual values.

Table 9 Sensitivity analysis of parameters pertaining to soil specifications.

Figure 1

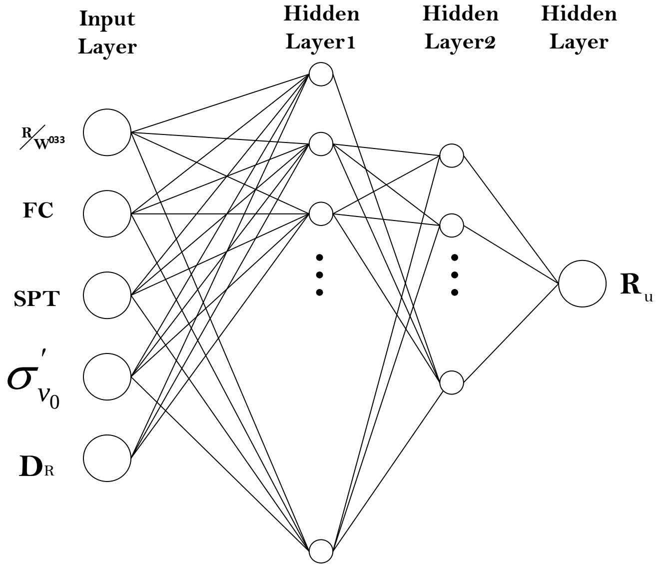

Input Layer
Hidden Layer1
Hidden Layer2
Hidden Layer
R/W033
FC
SPT
σ'_{v_0}
D_R
R_u

Figure 2

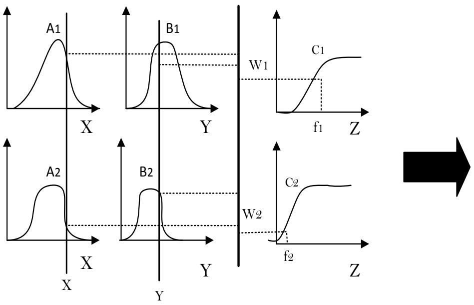

$$f = \frac{w_1 f_1 + w_2 f_2}{w_1 + w_2} = \bar{w}_1 f_1 + \bar{w}_2 f_2$$

Figure 3

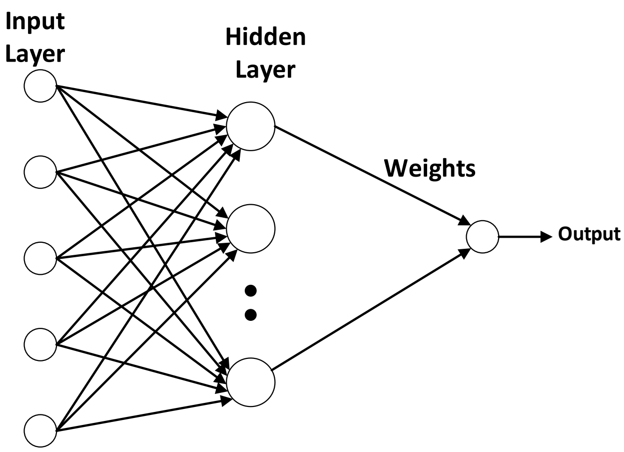

Figure 4

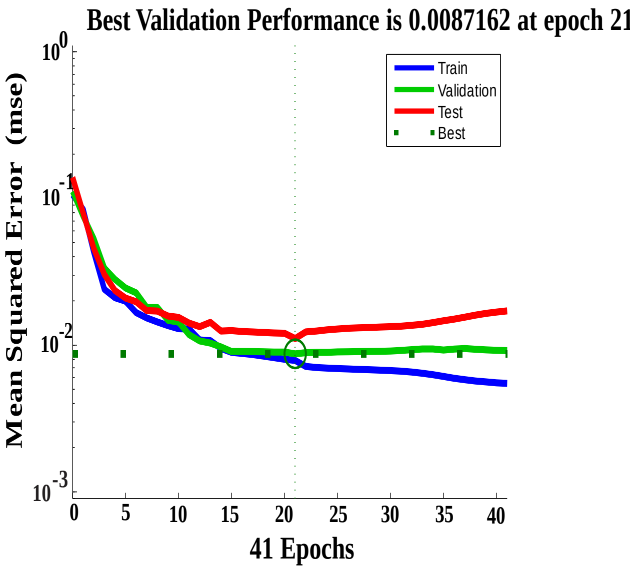

Figure 5

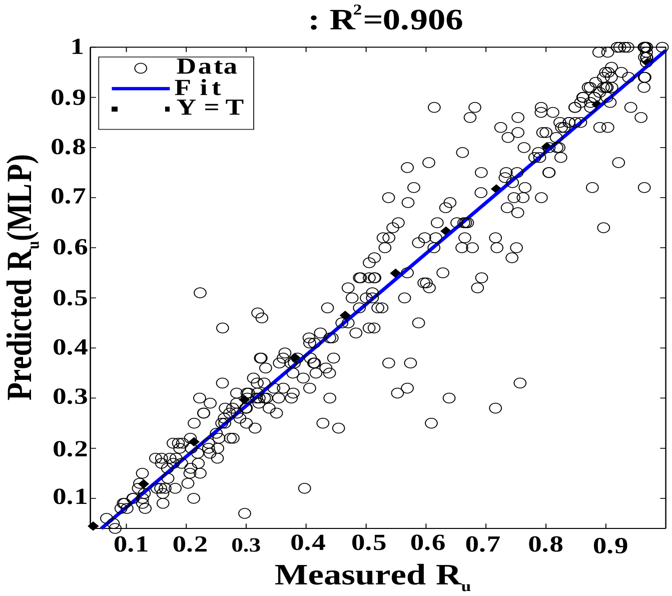
: R^2=0.906
Data
Fit
Y = T
Predicted R_u(MLP)
Measured R_u

(a)

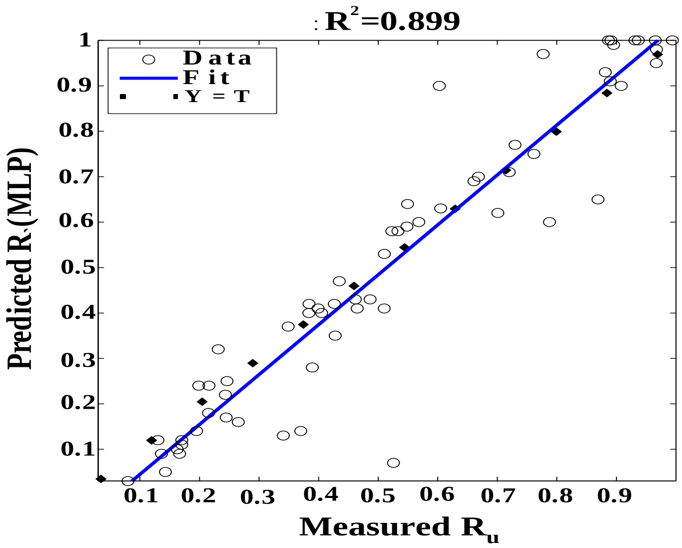
: R^2=0.899
Data
Fit
Y = T
Predicted R_u(MLP)
Measured R_u

(b)

Figure 6

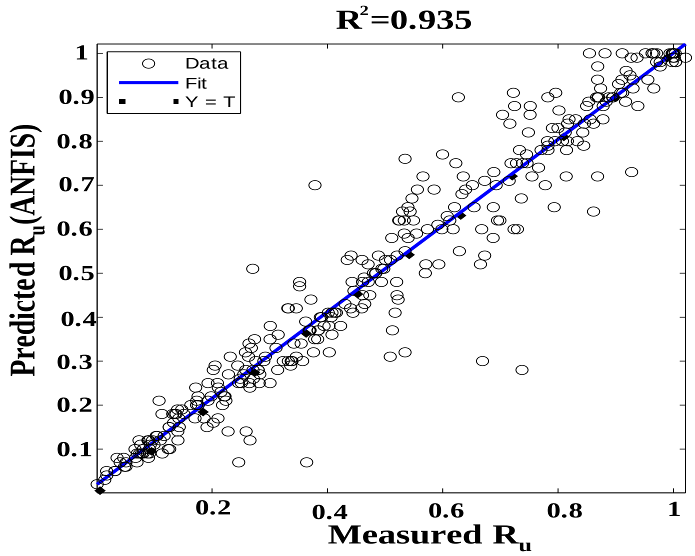

R^2=0.935
Data
Fit
Y = T
Predicted R_u(ANFIS)
Measured R_u
0.1
0.2
0.3
0.4
0.5
0.6
0.7
0.8
0.9
1
0.2
0.4
0.6
0.8
1

(a)

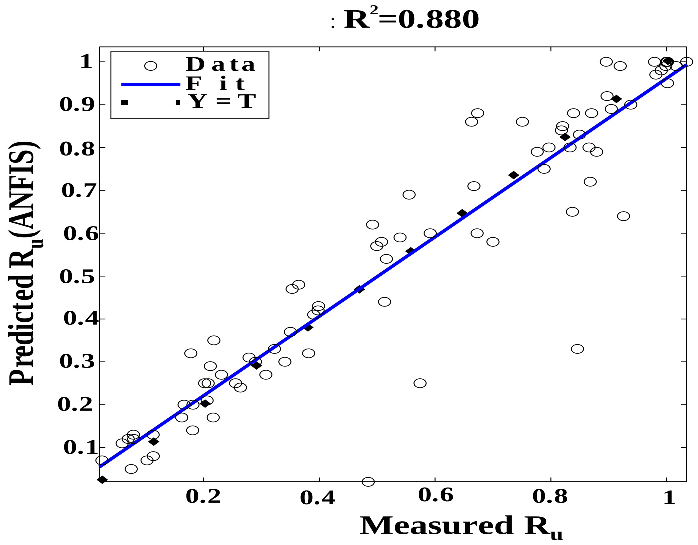

: R^2=0.880
Data
Fit
Y = T
Predicted R_u(ANFIS)
Measured R_u
0.1
0.2
0.3
0.4
0.5
0.6
0.7
0.8
0.9
1
0.2
0.4
0.6
0.8
1

(b)

Figure 7

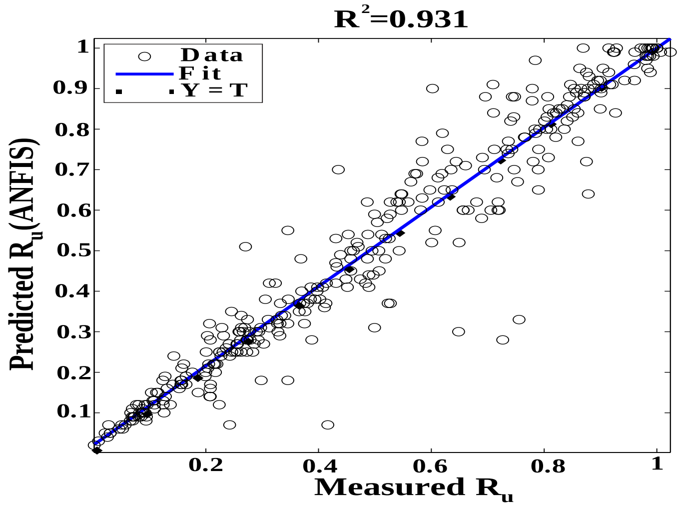

R^2=0.931
Data
Fit
Y = T
Predicted R_u(ANFIS)
Measured R_u

(a)

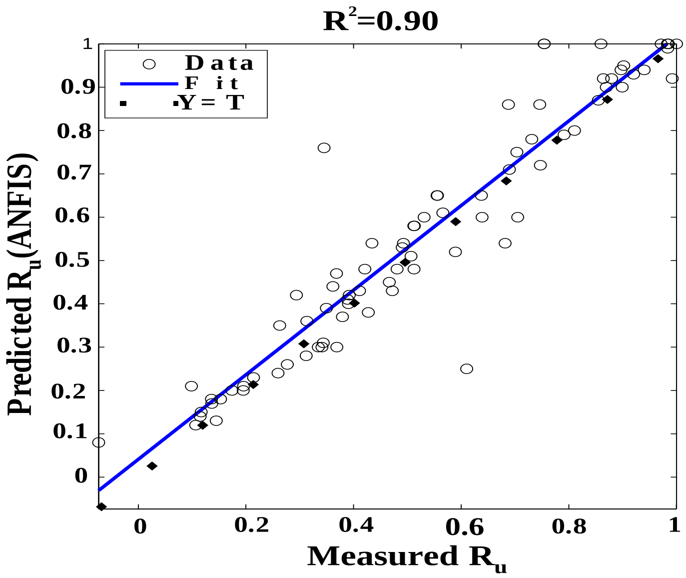

R^2=0.90
Data
Fit
Y = T
Predicted R_u(ANFIS)
Measured R_u

(b)

Figure 8

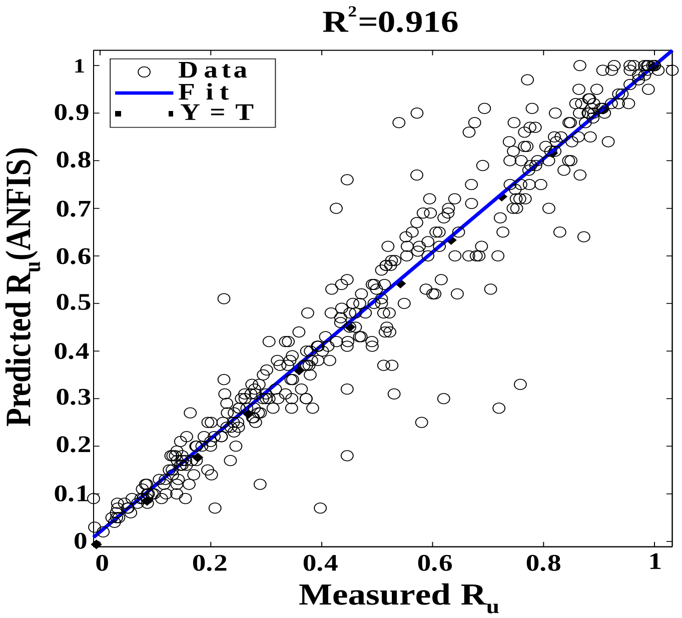
R²=0.916
Data
Fit
Y = T
Predicted Ru(ANFIS)
Measured Ru
0
0.1
0.2
0.3
0.4
0.5
0.6
0.7
0.8
0.9
1
0
0.2
0.4
0.6
0.8
1

(a)

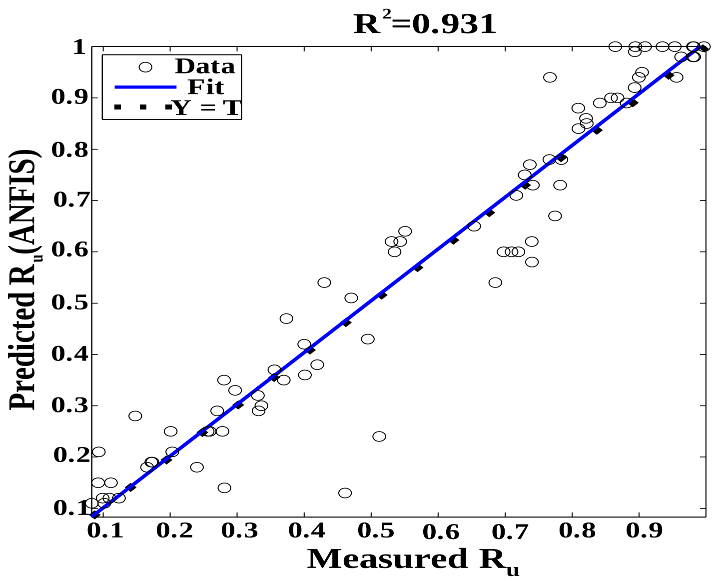
R²=0.931
Data
Fit
Y = T
Predicted Ru(ANFIS)
Measured Ru
0.1
0.2
0.3
0.4
0.5
0.6
0.7
0.8
0.9
1
0.1
0.2
0.3
0.4
0.5
0.6
0.7
0.8
0.9

(b)

Figure 9

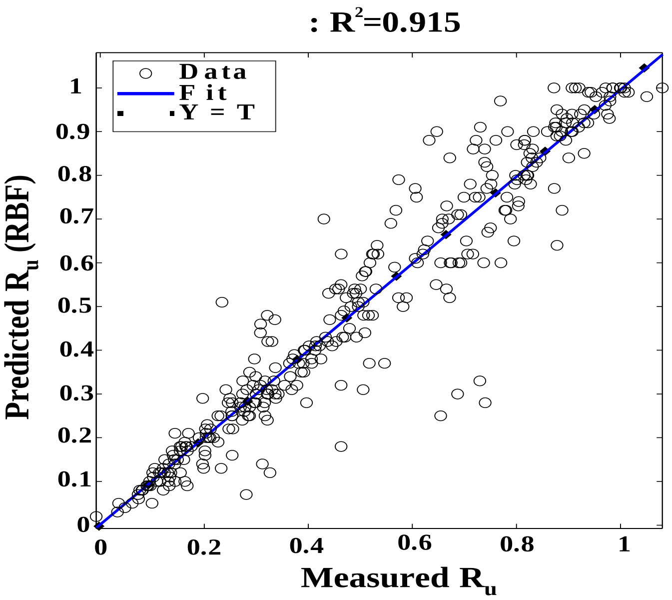

: R^2=0.915
Data
Fit
Y = T
Predicted R_u (RBF)
Measured R_u

(a)

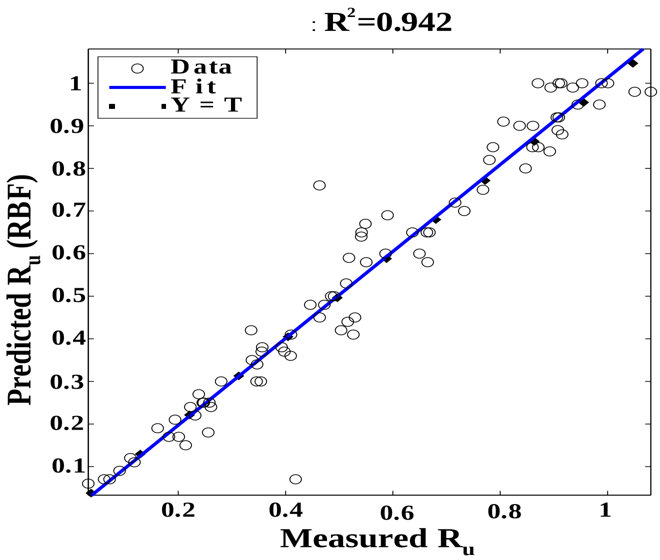

: R^2=0.942
Data
Fit
Y = T
Predicted R_u (RBF)
Measured R_u

(b)

Table 1

Parameter	Description
Type neural network	feed forward
Training algorithm	back propagation
Function error	mean square error(MSE)
Optimization method	Levenberg-Marquardt(LM)
Hidden layers	2
The number of neurons in the first hidden layer	15
The number of neurons in the second hidden layer	5
Transfer functions the hidden layer	tansig
Transfer functions the output layer	tansig
Number of training data	292 sample (70%)
Number of validation data	62 sample (15%)
Number of test data	62 sample (15%)

Table 2

Basic statistics	Input variables					Output variable R_u
	R/W0.33	SPT	σ'_{v_0}	D_R	FC	
Max	20.57	16	136	70	40	1
Min	1.78	1	13.60	12	5	0.02
Mean	6.05	7.49	70.54	31.83	7.57	0.52
SD	3.82	3.71	33.60	14.45	2.97	0.30

Comment [a34]: In response to comment 12 reviewer 2\

Table 3

	Predicted1	Predicted 0
True 1	TP	FN
True 0	FP	TN

Table 4

	R^2	RMSE	MAE	MAXAE
Training set	0.906	0.089	0.057	0.436
Testing set	0.899	0.105	0.07	0.456
Testing set	**PPV**	**TPR**	**TNR**	**ACCURACY**
	0.979	0.959	0.923	0.952

Table 5

	R^2	RMSE	MAE	MAXAE
Training set				
GP	0.935	0.076	0.049	0.435
SCM	0.931	0.079	0.05	0.447
FCM	0.916	0.086	0.054	0.44
Testing set				
GP	0.88	0.113	0.068	0.516
SCM	0.9	0.094	0.06	0.36
FCM	0.931	0.081	0.057	0.331
Testing set				
	PPV	**TPR**	**TNR**	**ACCURACY**
GP	0.953	0.909	0.852	0.89
SCM	1.000	0.952	1.000	0.950
FCM	1.000	0.982	1.000	0.988

Table 6

	R^2	RMSE	MAE	MAXAE
Training set	0.915	0.088	0.056	0.456
Testing set	0.942	0.06	0.042	0.202
Testing set	**PPV**	**TPR**	**TNR**	**ACCURACY**
	1	0.985	1	0.988

Table 7

	Field results		Network simulation		Regression analysis			Field results		Network simulation		Regression analysis	
	R_u	Liquefaction	R_u	Liquefaction	R_u	Liquefaction		R_u	Liquefaction	R_u	Liquefaction	R_u	Liquefaction
1	0.5	No	0.57	No	0.60	No	43	0.65	No	0.64	No	0.52	[illegible]
2	0.73	No	0.79	No	0.81	Yes	44	0.93	Yes	0.91	Yes	0.88	Yes
3	0.37	No	0.41	No	0.32	No	45	0.5	No	0.50	No	0.64	No
4	0.44	No	0.51	No	0.55	No	46	0.73	No	0.66	No	0.55	No
5	0.36	No	0.42	No	0.58	No	47	0.27	No	0.29	No	0.34	No
6	0.04	No	0.06	No	0.03	No	48	0.72	No	0.72	No	0.51	No
7	0.07	No	0.07	No	0.09	No	49	0.5	No	0.48	No	0.53	No
8	0.16	No	0.16	No	0.25	No	50	0.13	No	0.17	No	0.23	No
9	0.3	No	0.23	No	0.27	No	51	0.32	No	0.35	No	0.55	No
10	0.32	No	0.29	No	0.52	No	52	0.9	Yes	0.89	Yes	0.93	Yes
11	0.42	No	0.34	No	0.33	No	53	0.8	No	0.81	Yes	0.56	No
12	0.95	Yes	0.89	Yes	0.60	No	54	0.48	No	0.50	No	0.54	No
13	0.8	No	0.83	Yes	0.89	Yes	55	0.19	No	0.22	No	0.30	No
14	1	Yes	0.85	Yes	0.66	No	56	0.12	No	0.10	No	0.28	No
15	0.09	No	0.09	No	0.03	No	57	0.18	No	0.23	No	0.43	No
16	0.37	No	0.41	No	0.44	No	58	0.75	No	0.74	No	0.57	No
17	0.99	Yes	0.94	Yes	1.09	Yes	59	0.28	No	0.22	No	0.34	No
18	0.31	No	0.29	No	0.52	No	60	0.09	No	0.10	No	0.16	No
19	0.12	No	0.14	No	0.23	No	61	0.25	No	0.32	No	0.41	No
20	0.94	Yes	0.95	Yes	0.87	Yes	62	0.84	Yes	0.68	No	0.74	No
21	0.54	No	0.52	No	0.56	No	63	0.09	No	0.16	No	0.29	No
22	0.62	No	0.54	No	0.49	No	64	0.09	No	0.09	No	0.09	No
23	0.31	No	0.51	No	0.71	No	65	0.2	No	0.21	No	0.08	No
24	0.85	Yes	0.92	Yes	0.64	No	66	0.9	Yes	0.87	Yes	0.86	Yes
25	0.34	No	0.36	No	0.56	No	67	0.7	No	0.75	No	0.78	No
26	0.89	Yes	0.87	Yes	0.82	Yes	68	0.25	No	0.26	No	0.32	No
27	0.98	Yes	1.03	Yes	0.65	No	69	0.18	No	0.17	No	0.23	No
28	0.59	No	0.55	No	0.59	No	70	0.69	No	0.64	No	0.66	No
29	0.42	No	0.43	No	0.50	No	71	0.67	No	0.55	No	0.68	No
30	0.37	No	0.56	No	0.54	No	72	0.68	No	0.63	No	0.65	No
31	0.24	No	0.24	No	0.30	No	73	0.92	Yes	0.96	Yes	0.79	No
32	0.1	No	0.10	No	0.02	No	74	0.87	Yes	0.82	Yes	0.54	No
33	0.31	No	0.26	No	0.48	No	75	0.35	No	0.38	No	0.58	No
34	0.07	No	0.06	No	0.09	No	76	0.27	No	0.34	No	0.50	No
35	0.23	No	0.20	No	0.39	No	77	0.1	No	0.12	No	0.27	No
36	1	Yes	0.91	Yes	0.69	No	78	0.26	No	0.28	No	0.34	No
37	0.32	No	0.29	No	0.22	No	79	0.33	No	0.28	No	0.33	No
38	0.48	No	0.52	No	0.65	No	80	0.6	No	0.67	No	0.68	No
39	0.51	No	0.50	No	0.64	No	81	0.12	No	0.13	No	0.23	No
40	0.3	No	0.32	No	0.85	Yes	82	0.96	Yes	0.97	Yes	0.88	Yes
41	0.46	No	0.29	No	0.45	No	83	0.6	No	0.65	No	0.47	No
42	0.2	No	0.20	No	0.45	No							

Comment [a35]: In response to comment 12 reviewer 2

Table 8

	R_{u}-Observed	R_{u}-Predicted
Mean	0.468313	0.46878
Variance	0.085041	0.079251
Observations	83	83
Hypothesized Mean Difference	0	
Df	164	
t Stat	-0.01049	
P (T<=t)	0.991646	
t Critical	1.974535	

Table 9

.

	R^2	RMSE	MAE	MAXAE
The best ANN	0.966	0.06	0.042	0.202
ANN no SPT	0.895	0.094	0.063	0.392
ANN no σ'_{v_0}	0.903	0.087	0.066	0.200
ANN no DR	0.940	0.070	0.050	0.274
ANN no FC	0.930	0.073	0.054	0.227

Biographies

Fariba Asvar received B.S. degree in Civil Engineering from Shahid Bahonar Kerman University, Kerman, Iran, in 2011 and M.S. degree in Geotechnical Engineering from Yazd University, Yazd, Iran, in 2014. She is currently pursuing a Ph.D. degree in the field of Geotechnical Engineering at Yazd University, Yazd, Iran, since 2016. Her research interests include soil liquefaction, limit analysis in soil mechanics and application of neural networks in geotechnical engineering.

Arash Shirmohammadi **Faradonbeh** received B.S. degree in Civil Engineering from Sharekord, Islamic Azad University, Shahrekord, Iran in 2011, and M.S. degree in Geotechnical Engineering from Yazd University, Yazd, Iran, in 2014. He is currently pursuing a Ph.D. degree in the field of Geotechnical Engineering at kharazmi University, Tehran, Iran, since 2016. His research interests include Numerical modeling in Geotechnical Engineering especially blasting and liquefaction, soil-structure interaction and environmental geotechncs.

Kazem Barkhordari Bafghi received His MSc degree in Civil Engineering from Tehran University, Iran in 1986 and PhD degree in Geotechnical Engineering from the University of Surrey, UK, in 1998. He is currently Associate Professor in the Faculty of Civil Engineering at Yazd University, Iran. His research interests are foundation Engineering, earth dam and retaining structures.